NOTES AND CORRESPONDENCE

Generalized Adjoint for Physical Processes with Parameterized Discontinuities. Part V: Coarse-Grain Adjoint and Problems in Gradient Check

QIN XU

Naval Research Laboratory, Monterey, California

JIDONG GAO

CAPS, University of Oklahoma, Norman, Oklahoma

WEI GU

Department of Atmospheric Sciences, Nanjing University, Nanjing, China, and CIMMS, University of Oklahoma, Norman, Oklahoma

12 May 1997 and 19 September 1997

ABSTRACT

When on/off switches are triggered at discrete time levels by a threshold condition in a traditionally discretized model, the model solution is not continuously dependent on the initial state and this causes problems in tangent linearization and adjoint computations. It is shown in this paper that the problems can be avoided by introducing coarse-grain tangent linearization and adjoint without modifying the traditional discretization, although the coarse-grain gradient check can be performed only for finite perturbations.

1. Introduction

The classic adjoint formulations were generalized by Xu (1996a,b; 1997a) for physical processes with parameterized discontinuities. According to the recent study of Xu (1997b), in order to apply the generalized adjoint formulations to time discrete numerical models, the traditional time discretization scheme needs to be modified with the switch time determined by interpolation as a continuous function of the initial state. Otherwise, the discrete solution is not continuously dependent on the initial state and, consequently, the cost function contains zigzag discontinuities and their gradients contain delta functions. These delta functions are accurate descriptions of the local jumps of the cost function with respect to infinitesimal perturbations of the initial state, but they cannot tell the ''nonlocal'' variations of the cost function with respect to finite perturbations of the initial state. Since practical adjoint applications consider finite perturbations, the central problem here concerns how to estimate the coarse-grain gradient for the nonlocal variations of the cost function. This problem can be solved, as proposed in Xu (1997b), by modifying the traditional time discretization so that the computed gradient contains no delta function and can be used for nonlocal variations. This approach is clean but requires additional work in modifying the existing forward model. If the forward model is not modified, then an alternate approach is needed to compute the coarse-grain gradient. The related problems will be examined in this paper.

The paper is organized as follows. The analytical benchmark model and two types of discrete forward models are reviewed in the following section. Detailed error analyses are performed in section 3 for four types of tangent linear models derived from the two discrete forward models. Adjoint models and problems in gradient check are examined in section 4. The results are summarized with conclusions in section 5.

2. Review of analytical model and two types of discrete forward models

a. Analytical model and benchmark solutions

As in Xu (1996a, hereafter referred to as X96a) and Xu (1997b, hereafter referred to as X97b), the analytical model is described by the following equation:

$$d_t x = F + H(x - x_c)G,$$
$$x = x_0 \quad \text{at} \quad t = 0, \tag{2.1}$$

Corresponding author address: Dr. Qin Xu, Naval Research Laboratory, 7 Grace Hopper Drive, Monterey, CA 93943-5502.
E-mail: xuq@helium.nrlmry.navy.mil

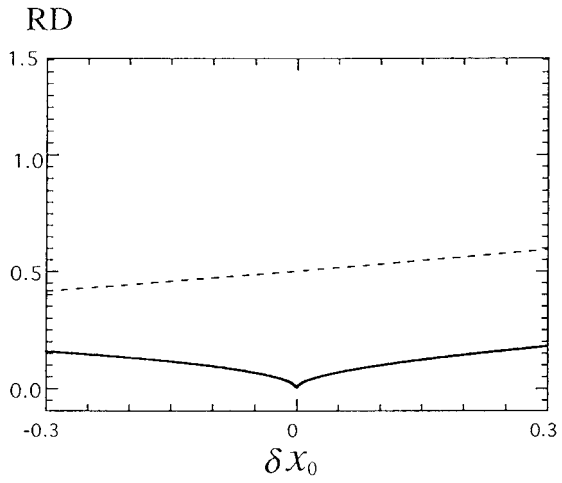

FIG. 1. Relative difference [*RD* defined in (2.2)] between analytical tangent linear solution δx and nonlinear perturbation Δx. Solid and dashed curves are for the generalized and conventional tangent linear solutions, respectively. The parameter values are $F = 1$, $G = -0.5$, $x_c = 0.38$, and $T = 1$.

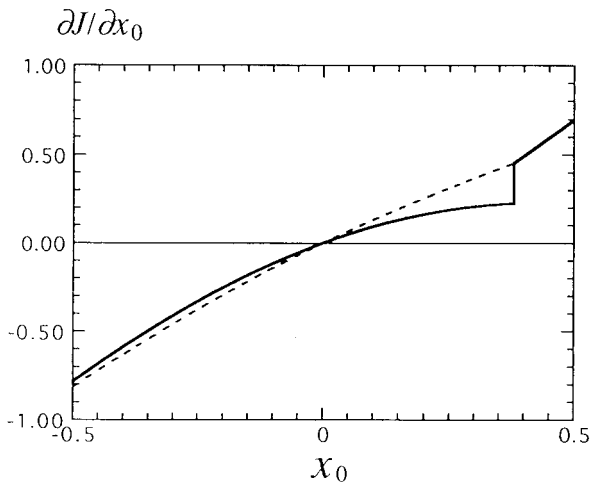

FIG. 2. Analytical gradient $\partial J/\partial x_0$ (solid curve) and conventional adjoint solution (dashed curve). The parameter values are as in Fig. 1.

where G and F are constant, $H(\ )$ is the Heaviside unit-step function (see p. 622 of Courant and Hilbert 1962), and x_c is the threshold value for the parameterized process. As shown in X96a, $H(x - x_c)$ can be replaced by $H(t - \tau)$ for an on-switch or by $H(\tau - t)$ for an off-switch, where τ denotes the switch time.

The generalized tangent linear equation of (2.1) is given by $d_t\delta x = \delta x H'(t - \tau)G/F$ [see (3.7) of X96a or (2.3a) of X97b]. As shown in X96a, the solution of this generalized tangent linear equation is the first-order approximation of the nonlinear perturbation $\Delta x = x' - x$, where x' is perturbed solution obtained from (2.1) with x_0 replaced by $x_0 + \delta x_0$. The relative difference (RD) between δx and Δx can be measured by

$$\mathrm{RD} = \left[\int_0^T (\delta x - \Delta x)^2\, dt\right]^{1/2}\left[\int_0^T (\Delta x)^2\, dt\right]^{-1/2}. \quad (2.2)$$

Since δx and Δx are functions of δx_0, RD is also a function of δx_0. As shown by the solid curve in Fig. 1 (with $F = 1$, $G = -0.5$, $x_c = 0.38$, $x_0 = 0$, and $T = 1$), RD $\approx O(\delta x_0)$, so the generalized tangent linear solution δx is a valid linear approximation of the nonlinear perturbation Δx.

The conventional tangent linear equation of (2.1) is given by $d_t\delta x = 0$ (see case 1 in section 3a of X96a), and the solution is given by $\delta x = \delta x_0$. The relative difference (RD) between this solution $\delta x = \delta x_0$ and the nonlinear perturbation Δx is shown by the dashed curve in Fig. 1. Unlike the solid curve, this dashed curve is far above zero even when δx_0 becomes zero, so the conventional tangent linear solution is not a valid linear approximation of Δx.

The analytical cost function has the following form:

$$J = \int_0^T D^2\, dt, \quad (2.3)$$

where $D = x - x_{\mathrm{ob}}$, x is the solution of (2.1), and x_{ob} is the observed value of x, which is error free and given by the analytical solution of (2.1) with $x_0 = 0$. Substituting the solution of (2.1) into (2.3) gives an analytical expression of the cost function [see (6.7) and Fig. 9 of X96a]. The gradient of this cost function, $\partial J/\partial x_0$, is plotted by the solid curve in Fig. 2. This gradient can be exactly derived by the backward integration of the generalized adjoint equation [see (3.8) of X96a or section 2 of X97b], but not by the backward integration of the conventional adjoint equation [see (3.3) of X96a]. The conventional adjoint solution is plotted by the dashed curve in Fig. 2, which is clearly different from the true gradient (solid curve). These analytical results will be used as benchmarks for the numerical experiments in the subsequent sections.

b. FM0—Traditional time discretization of the forward model

As in (3.1) of X97b, the traditional discretization of (2.1) yields the following forward model (FM0):

$$\begin{aligned} x_n &= x_{n-1} + F\Delta t && \text{for } n = 1, 2, \cdots, m, \\ x_n &= x_{n-1} + (F + G)\Delta t && \text{for } n = m + 1, \\ & && \quad m + 2, \cdots, N, \end{aligned} \quad (2.4)$$

where $\Delta t = T/N$ is the time step. Here, an on-switch is triggered at the mth level immediately after the threshold condition is exceeded, and this mth time level is determined by $x_m \geq x_c > x_{m-1}$.

The discrete cost function has the following form:

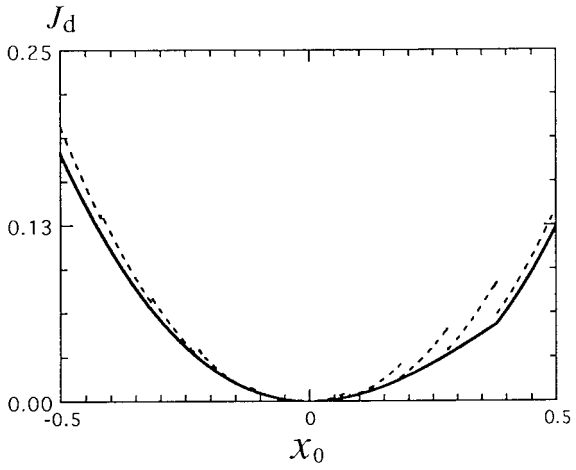

FIG. 3. Costfunction J_d constrained by FM0 (dashed) or by FM1 (solid). Here, $N = 10$ (or $\Delta t = 0.1$) is used for the discrete models FM0 and FM1. The parameter values are as in Fig. 1.

$$J_d = \sum_{n=0}^{N} D_n^2 \Delta t, \tag{2.5}$$

where $D_n = x_n - x_{obn}$ and x_{obn} is observed value of x at the nth time level, which, as in (2.3), is error free and given by the analytical solution of (2.1) with $x_0 = 0$. As explained in X97b, the FM0 solution is not continuously dependent on the initial state x_0 (see Fig. 2 of X97b), and this causes zigzag discontinuities in J_d (see the dashed curve in Fig. 3). As these discontinuities cause delta functions in the gradient (see Fig. 3 of X97b), the derived gradient $\partial J_d/\partial x_0$ can be very different from the analytical one $\partial J/\partial x_0$.

c. *FM1—Modified time discretization of the forward model*

The above problem can be solved if the traditional discretization is modified with the switch time determined by linear interpolation as a continuous function of the initial state. The modified forward model (FM1) is given in (5.1) of X97b. Since the FM1 solution is continuously dependent on the initial state x_0, the cost function J_d now is a continuous function of x_0 (see the solid curve in Fig. 3). As shown in section 5 of X97b, when $\Delta t \to 0$, $J_d \to J$ and $\partial J_d/\partial x_0 \to \partial J/\partial x_0$, so $\partial J_d/\partial x_0$ is a good approximation of the analytical gradient $\partial J/\partial x_0$.

3. Four types of tangent linear models

a. *CTLM0—Conventional tangent linearization of FM0*

As the switch time variation is ignored, the conventional tangent linearization of FM0 in (2.4) yields (CTLM0)

$$\delta x_n = \delta x_{n-1} \quad \text{for} \quad n = 1, 2, \cdots, N. \tag{3.1}$$

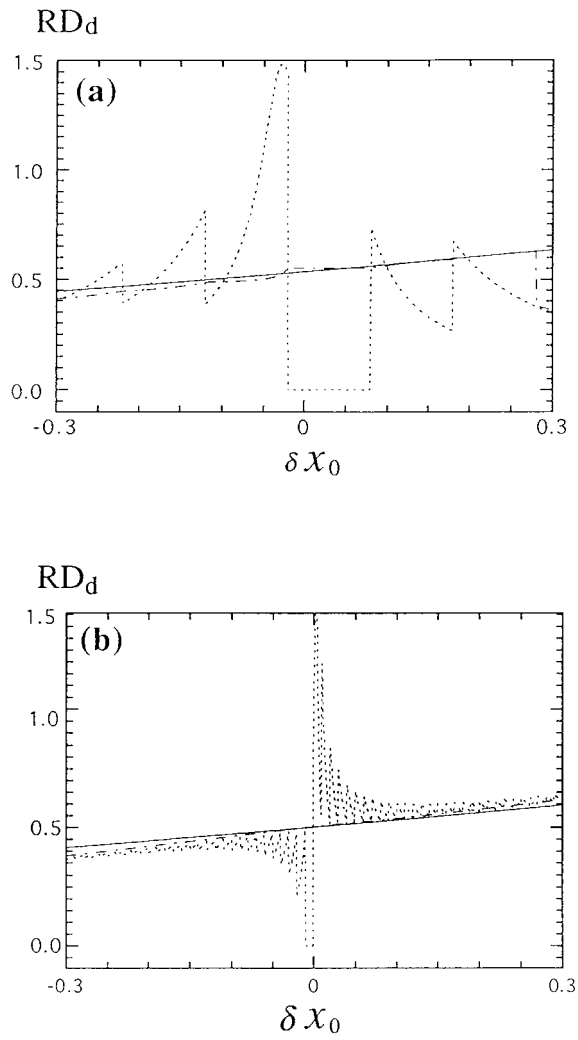

FIG. 4. As in Fig. 1 except for two RD_d curves [see (3.2)]: the dotted with δx_n computed by CTLM0 and Δx_n obtained from FM0, and the dashed with δx_n computed by CTLM1 and Δx_n obtained from FM1. The thin solid line is the same as the dashed analytical curve in Fig. 1. Here, $N = 10$ is used in (a), and $N = 100$ is used in (b).

The solution of (3.1) is a trivial one: $\delta x_n = \delta x_0$ and is very different from the nonlinear perturbation $\Delta x_n = x_n' - x_n$, where x_n' is the solution obtained from (2.4) with the perturbed initial state $x_0 + \delta x_0$. The relative difference between δx_n and Δx_n can be measured by

$$\mathrm{RD}_d = \left[\sum_{n=0}^{N} (\delta x_n - \Delta x_n)^2\right]^{1/2} \left[\sum_{n=0}^{N} (\Delta x_n)^2\right]^{-1/2}. \tag{3.2}$$

As shown by the dotted curve in Fig. 4a (where $N = 10$ and $\Delta t = 0.1$), $RD_d = 0$ when the initial perturbation δx_0 is within a small range (determined by $F\Delta t = 0.1$) in the vicinity of zero. In this case, the initial perturbation δx_0 is too small to cause the switch time to jump from one time level to the next time level (see Fig. 3 of X97b), so $\Delta x_n = \delta x_n = \delta x_0$ and $RD_d = 0$.

When δx_0 moves beyond the above small range, the switch time jumps and Δx_n and RD_d also jump. As shown in Fig. 4a, the dotted RD_d curve jumps every time when δx_0 is changed by $F\Delta t$. According to (2.4) the jump of Δx_n is proportional to $G\Delta t$, and according to (3.2) the jump of RD_d is proportional to $G\Delta t/\delta x_0$. When Δt is small, as shown in Fig. 4b, the jumps of the dotted RD_d curve become small and densely packed. When $\Delta t \to 0$, the dotted RD_d curve approaches (for $\delta x_0 \neq 0$) to the analytical *RD* curve far above zero (shown by thin solid line in Fig. 4b and dashed line in Fig. 1). Thus, when $|\delta x_0| \geq O(F\Delta t)$, the CTLM0 solution is not a valid approximation of the nonlinear perturbation obtained from FM0. When $|\delta x_0| < O(F\Delta t)$ and $RD_d = 0$, the CTLM0 solution is the same as the nonlinear perturbation obtained from FM0, but the latter is not a valid discrete approximation of the analytical nonlinear perturbation obtained from (2.1).

b. CTLM1—Conventional tangent linearization of FM1

The conventional tangent linearization of FM1 yields CTLM1, which has the same form as CTLM0 in (3.1). The CTLM1 solution is also a trivial one: $\delta x_n = \delta x_0$. The relative difference RD_d between this CTLM1 solution and the nonlinear perturbation Δx_n obtained from FM1 (instead of FM0) is plotted by the dashed curves in Figs. 4a,b. These dashed RD_d curves are very close to the analytical *RD* curve for the conventional tangent linearization (shown by thin solid line in Fig. 4 and dashed line in Fig. 1). That these curves are far above zero indicates that CTLM1 is not a valid tangent linear model of FM1.

c. GTLM1—Generalized tangent linearization of FM1

The generalized tangent linearization of FM1 yields GTLM1, and the detailed formulation is given in (5.5) of X97b. The relative difference RD_d between the GTLM1 solution and the nonlinear perturbation Δx_n obtained from FM1 is plotted by the dashed curve in Fig. 5. This dashed RD_d curve is very close to the analytical *RD* curve for the generalized tangent linearization (shown by thin solid line in Fig. 5 and thick solid line in Fig. 1). Since $RD_d \approx RD \approx O(\delta x_0)$, the GTLM1 solution is a good linear approximation of the nonlinear perturbation obtained from FM1.

d. GCTLM0—Generalized coarse-grain tangent linearization of FM0

The generalized tangent linearization of FM0 can be derived, but the derived solution contains delta functions [see (4.2) of X97b] and thus is not a good approximation of the nonlinear perturbation of the FM0 solution. In this case, for practical applications, we need to consider the so-called generalized coarse-grain tangent linearization of FM0, denoted by GCTLM0, for finite perturbations. This GCTLM0 can be obtained by directly discretizing the analytical generalized tangent linear equation of (2.1) [see (3.7) of X96a or (2.3a) of X97b], while the impact of the delta function in the analytical equation at the switch point (between time levels $m-1$ and m) can be computed by

$$\int_{(m-1)\Delta t}^{m\Delta t} H'(t-\tau)\delta x\, dt = \delta x(\tau_-) \approx \delta x_{m-1}. \quad (3.3)$$

One can verify that the derived GCTLM0 has the same form as GTLM1 [see (5.5) of X97b] for the simple example considered in this paper. In general, GCTLM0 can be different from GTLM1 in the high-order terms.

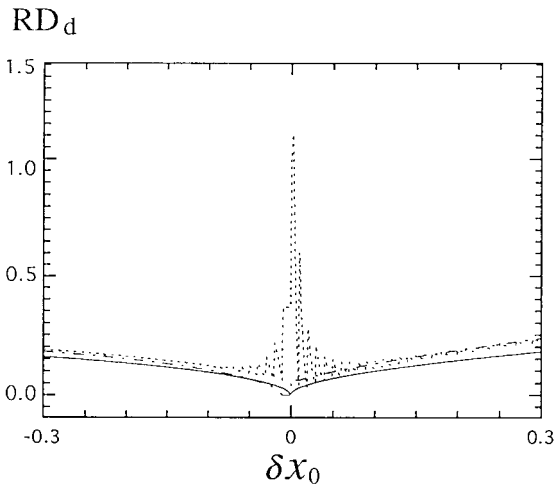

FIG. 5. As in Fig. 4b except the dotted curve is obtained with δx_n computed by GCTLM0 and Δx_n obtained from FM0, and the dashed curve is obtained with δx_n computed by GTLM1 and Δx_n obtained from FM1.

The relative difference (RD_d) between the GCTLM0 solution and the nonlinear perturbation obtained from FM0 is plotted by the dotted curves in Fig. 5 for $\Delta t = 0.01$. As shown, RD_d has large jumps when $|\delta x_0| \leq O(F\Delta t)$. These jumps are caused by the noncontinuous dependence of the nonlinear perturbation on the initial perturbation δx_0. The situation is similar to that in Fig. 4b, except that the jumps in Fig. 4b are rooted on a different analytical *RD* curve, which is far above zero (also see the dashed in Fig. 1). As $|\delta x_0|$ increases beyond $O(F\Delta t)$, the jumps on the RD_d curve diminish rapidly and the curve becomes very close to the solid analytical *RD* curve. This implies that GCTLM0 can be used as a coarse-grain tangent linear model of FM0 when the concerned finite perturbation is sufficiently larger than the change of the FM0 solution caused by one step jump of the switch time, that is, $|x_0' - x_0| \gg F\Delta t$ (see Fig. 3 of X97b). The adjoint of GCTLM0 can be used to compute the nonlocal gradient for the coarse-grain geometry of the cost function J_d constrained by FM0. The related problems are examined in the next section.

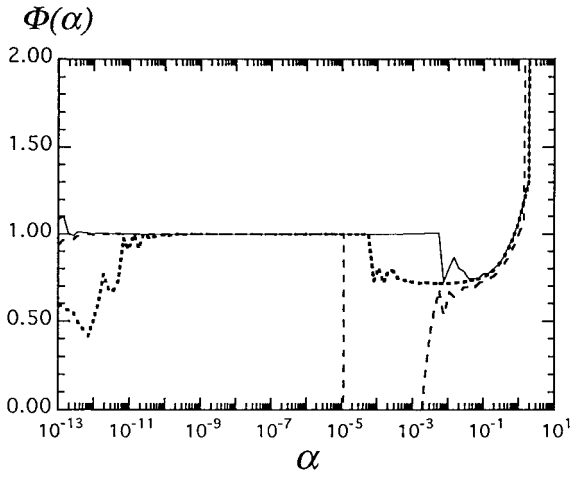

FIG. 6. Plots of $\Phi(\alpha)$ with gradient computed by the adjoint of CTLM0 and cost function computed by FM0 for three different cases: $x_0 = 0.1$ with $\Delta t = 0.001$ (solid), $x_0 = 0.129\ 998$ with $\Delta t = 0.001$ (dashed), and $x_0 = 0.1$ with $\Delta t = 0.000\ 01$ (dotted).

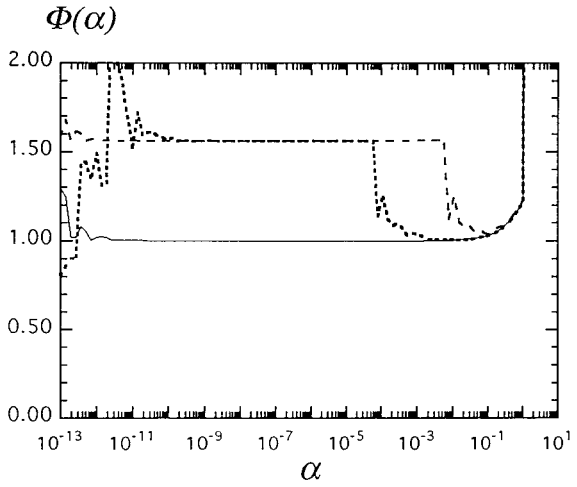

FIG. 7. Plots of $\Phi(\alpha)$ for three different cases: $\Delta t = 0.001$ (solid) with gradient computed by the adjoint of GTLM1 and cost function computed by FM1 at $x_0 = 0.2$, $\Delta t = 0.001$ (dashed), and $\Delta t = 0.000\ 01$ (dotted), with gradient computed by the adjoint of GCTLM0 and cost function computed by FM0 at $x_0 = 0.2$.

4. Adjoint models and problems in gradient check

The accuracy of a tangent linear model determines the accuracy of its adjoint. In this sense, the results presented for the four types of tangent linear models in the previous section have the following implications for their associated adjoint models. When the cost function J_d is constrained by FM1, the gradient $\partial J_d/\partial x_0$ can be accurately computed by the adjoint of GTLM1, but not by the adjoint of CTLM1. When the cost function J_d is constrained by FM0, the local gradient $\partial J_d/\partial x_0$ can be computed by the adjoint of CTLM0 if the initial state x_0 is not at a discontinuous point of the cost function $J_d(x_0)$. The gradient computed by this adjoint, however, is local and does not describe the coarse-grain geometry of the cost function constrained by FM0. On the other hand, the gradient computed by the adjoint of GCTLM0 is ''nonlocal'' and describes the coarse-grain geometry of the cost function constrained by FM0. For the example considered in this paper, the adjoint of GCTLM0 is exactly the same as the adjoint of GTLM1, so their solutions give the same gradient—the gradient of the cost function constrained by FM1. This cost function (shown by the solid curve in Fig. 3) now is treated by the adjoint of GCTLM0 as the coarse-grain geometry of the cost function constrained by FM0 (shown by the dashed curve in Fig. 3).

The solution of the adjoint of GCTLM0 captures the nonlocal impacts of the delta functions in the gradient of the cost function constrained by FM0, but it does not match the spikes of the delta functions. Thus, there are problems concerning how the gradients computed by the adjoints of CTLM0 and GCTLM0 should be checked numerically against the direct perturbations of the FM0 solutions. Normally, the accuracy of the gradient computed by adjoint integration can be checked by the following formula:

$$\Phi(\alpha) = [J_d(x_0 + \alpha u) - J_d(x_0)]/[\alpha u \partial J_d/\partial x_0] = 1 + O(\alpha), \quad (4.1)$$

where $u = (\partial J_d/\partial x_0)|\partial J_d/\partial x_0|^{-1}$ and $0 < \alpha \ll 1$. When α is small but not as small as the machine round-off error, one should expect that $\Phi(\alpha) = 1 + O(\alpha)$, and the result should not be very much dependent on x_0. This, however, is not the case for the gradient computed by the adjoint of CTLM0. As shown in Fig. 6, when the gradient is computed at $x_0 = 0.1$ by the adjoint of CTLM0 with $\Delta t = 0.001$, the $\Phi(\alpha)$ curve (solid) is closely along 1 over the wide range of $10^{-12} < \alpha < 4 \times 10^{-3}$, but drops suddenly as α increases to 4×10^{-3}. This problem is caused by the noncontinuous dependence of the FM0 solution on the initial condition $x_0 + \alpha u$. There is no jump in the FM0 solution until α reaches 4×10^{-3}. Once α increases to 4×10^{-3}, the switch time jumps to the next discrete time level, and thus the solid $\Phi(\alpha)$ curve drops suddenly. When the time step becomes as small as $\Delta t = 0.000\ 01$, the $\Phi(\alpha)$ curve (dotted) drops even as early as α just increases to 5×10^{-5}. The switch time is affected not only by α and Δt but also by the initial state x_0. When x_0 is very close to a discontinuous point of $J_d(x_0)$, a very small α can cause the switch time to jump. For example, when $x_0 = 0.129\ 998$ and $\Delta t = 0.001$, the $\Phi(\alpha)$ curve (dashed line in Fig. 6) drops dramatically even as α just increases to 10^{-5}. Thus, depending on the reference initial state x_0, the gradients computed by the adjoint of CTLM0 can give very different $\Phi(\alpha)$ curves.

The gradient computed by the adjoint of GTLM1 can be checked by (4.1) to great precision, and the result is shown by the solid $\Phi(\alpha)$ curve in Fig. 7. This result is independent of x_0. The gradient computed by the adjoint of GCTLM0, however, cannot be accurately checked by

(4.1). As shown by the dashed curve in Fig. 7, $\Phi(\alpha)$ (computed with $\Delta t = 0.001$) is significantly larger than 1 when $\alpha < 10^{-2}$. However, when α is between 10^{-2} and 5×10^{-1}, this dashed $\Phi(\alpha)$ curve is much closer to 1 than the three $\Phi(\alpha)$ curves in Fig. 6. Clearly, there is a finite range of α in which the $\Phi(\alpha)$ curve computed by the adjoint of GCTLM0 is much closer to 1 than that computed by the adjoint of CTLM0. This finite range expands leftward (to 5×10^{-5}) as Δt decreases (to 0.000 01), as shown by the dotted $\Phi(\alpha)$ curve in Fig. 7. When the initial perturbation δx_0 is in this finite range, the variation of J_d, that is, $\Delta J_d = J_d(x_0 + \alpha u) - J_d(x_0)$, can be well estimated by using the adjoint of GCTLM0 but not the adjoint of CTLM0. Thus, the former can be considered as a coarse-grain adjoint for FM0 and used to compute the coarse-grain gradient of the zigzag-discontinuous cost function constrained by FM0. This coarse-grain property is tied up with the coarse-grain property of GCTLM0 illustrated in the previous section.

5. Conclusions

When parameterized on/off switches are triggered at discrete time levels by a threshold condition in a numerical model, the switch time and thus the model solution are not continuously dependent on the initial state. This causes problems in tangent linearization of the discrete model and in computations of the cost function gradient (since the cost function contains small zigzag discontinuities). As shown in X97b, the problems can be solved by modifying the traditional time discretization. As a supplement of X97b, this study shows that the problems can be avoided by introducing coarse-grain tangent linearization and adjoint without modifying the traditional time discretization. The new results obtained in this paper are summarized as follows:

1) A coarse-grain tangent linear model can be derived by directly discretizing the analytical form of the generalized tangent linear equation without modifying the traditional discretization in the forward model. The coarse-grain tangent linear solution can be a valid approximation of the nonlinear perturbation obtained from the forward numerical model as long as the initial perturbation is sufficiently large to move the switch time through a large number of time levels (but not too large to cause severe nonlinearity).
2) The adjoint of the coarse-grain tangent linear model is a coarse-grain adjoint model. Both the coarse-grain adjoint and the conventional adjoint have problems with gradient check [see (4.1)], but the problems occur over different ranges of perturbation amplitude (see Figs. 6–7). When the time step is sufficiently small ($\Delta t \ll |x_0' - x_0|/F$, see Fig. 3 of X97b), the coarse-grain adjoint model can be used to compute the coarse-grain gradient of the zigzag-discontinuous cost function constrained by the traditionally discretized model.

Acknowledgments. This work was supported by NOAA Grant NA67Jo150 and NSF Grant ATM-9417304 to CIMMS and NSF Grant ATM91-20009 to CAPS at the University of Oklahoma and by the Office of Naval Research (ONR), Program Element 0602435N to the Marine Meteorology Division of the Naval Research Laboratory at Monterey.

REFERENCES

Courant, R., and D. Hilbert, 1962: *Methods of Mathematical Physics.* Vol. II. Interscience, 830 pp.

Xu, Q., 1996a: Generalized adjoint for physical processes with parameterized discontinuities. Part I: Basic issues and heuristic examples. *J. Atmos. Sci.,* **53,** 1123–1142.

——, 1996b: Generalized adjoint for physical processes with parameterized discontinuities. Part II: Vector formulations and matching conditions. *J. Atmos. Sci.,* **53,** 1143–1155.

——, 1997a: Generalized adjoint for physical processes with parameterized discontinuities. Part III: Mutiple threshold conditions. *J. Atmos. Sci.,* **54,** 2713–2721.

——, 1997b: Generalized adjoint for physical processes with parameterized discontinuities. Part IV: Problems in time discretization. *J. Atmos. Sci.,* **54,** 2722–2728.